



Swansea University
Prifysgol Abertawe



Cronfa - Swansea University Open Access Repository

This is an author produced version of a paper published in:

Ecology

Cronfa URL for this paper:

<http://cronfa.swan.ac.uk/Record/cronfa48011>

Paper:

Wells, K., Hamede, R., Jones, M., Hohenlohe, P., Storfer, A. & McCallum, H. (2019). Individual and temporal variation in pathogen load predicts long-term impacts of an emerging infectious disease. *Ecology*, 100(3), e02613

<http://dx.doi.org/10.1002/ecy.2613>

This item is brought to you by Swansea University. Any person downloading material is agreeing to abide by the terms of the repository licence. Copies of full text items may be used or reproduced in any format or medium, without prior permission for personal research or study, educational or non-commercial purposes only. The copyright for any work remains with the original author unless otherwise specified. The full-text must not be sold in any format or medium without the formal permission of the copyright holder.

Permission for multiple reproductions should be obtained from the original author.

Authors are personally responsible for adhering to copyright and publisher restrictions when uploading content to the repository.

<http://www.swansea.ac.uk/library/researchsupport/ris-support/>

1 **Individual and temporal variation in pathogen load predicts long-**
2 **term impacts of an emerging infectious disease**

3 Konstans Wells^{1,2,6}, Rodrigo K. Hamede³, Menna E. Jones³, Paul A. Hohenlohe⁴, Andrew
4 Storfer⁵, Hamish I. McCallum²

5

6 *1 Department of Biosciences, Swansea University, Singleton Campus, Wallace Building,*
7 *Swansea SA2 8PP, UK.*

8 *2 Environmental Futures Research Institute, Griffith University, Brisbane QLD 4111,*
9 *Australia.*

10 *3 School of Biological Sciences, University of Tasmania, Hobart, Tasmania 7001, Australia.*

11 *4 Institute for Bioinformatics and Evolutionary Studies, Department of Biological Sciences,*
12 *University of Idaho, Moscow, ID 83844, USA.*

13 *5 School of Biological Sciences, Washington State University, Pullman, WA 99164-4236*
14 *USA.*

15

16 6 E-mail: k.l.wells@swansea.ac.uk

17

18 **Running head: Tasmanian devil facial tumour disease**

19

20

21

22

23

24

25

26 ABSTRACT

27 Emerging infectious diseases increasingly threaten wildlife populations. Most studies focus
28 on managing short-term epidemic properties, such as controlling early outbreaks. Predicting
29 long-term endemic characteristics with limited retrospective data is more challenging. We
30 used individual-based modelling informed by individual variation in pathogen load and
31 transmissibility to predict long-term impacts of a lethal, transmissible cancer on Tasmanian
32 devil (*Sarcophilus harrisii*) populations. For this, we employed Approximate Bayesian
33 Computation to identify model scenarios that best matched known epidemiological and
34 demographic system properties derived from ten years of data after disease emergence,
35 enabling us to forecast future system dynamics. We show that the dramatic devil population
36 declines observed thus far are likely attributable to transient dynamics (initial dynamics after
37 disease emergence). Only 21% of matching scenarios led to devil extinction within 100 years
38 following devil facial tumour disease (DFTD) introduction, whereas DFTD faded out in 57%
39 of simulations. In the remaining 22% of simulations, disease and host coexisted for at least
40 100 years, usually with long-period oscillations. Our findings show that pathogen extirpation
41 or host-pathogen coexistence are much more likely than the DFTD-induced devil extinction,
42 with crucial management ramifications. Accounting for individual-level disease progression
43 and the long-term outcome of devil-DFTD interactions at the population-level, our findings
44 suggest that immediate management interventions are unlikely to be necessary to ensure the
45 persistence of Tasmanian devil populations. This is because strong population declines of
46 devils after disease emergence do not necessarily translate into long-term population declines
47 at equilibria. Our modelling approach is widely applicable to other host-pathogen systems to
48 predict disease impact beyond transient dynamics.

49

50

51 **KEYWORDS**

52 disease burden; long-periodicity oscillation; population viability; Tasmanian devil;
53 transmissible cancer; wildlife health

54

55 **INTRODUCTION**

56 Emerging infectious diseases most often attract attention because their initial impacts on host
57 populations are frequently severe (de Castro and Bolker 2005, Smith et al. 2009). Following
58 the initial epidemic and transient dynamic behaviour, long-term outcomes include pathogen
59 fadeout, host extinction, or long-term endemicity with varying impacts on the host population
60 size (Hastings 2004, Benton et al. 2006, Cazelles and Hales 2006). Predicting which of these
61 long-term outcomes may occur on the basis of initial transient dynamics is very challenging
62 and conclusions about possible disease effects on population viability based on early
63 epidemic dynamics can be misleading with regard to long-term dynamics. For example,
64 disease spread in a newly exposed population may slow down after reduction of the pool of
65 susceptible individuals and coevolutionary processes between a pathogen's virulence and host
66 defence mechanism may further impact long-term dynamics.

67

68 Nevertheless, predicting the long-term consequences of an infectious disease as early
69 as possible in the emergence process is important for management. If the disease has a high
70 likelihood of ultimately leading to host extinction, then strategies such as stamping out
71 infection by removing all potentially infectious individuals may be justifiable, despite short-
72 term impacts on the host species and ethical considerations (McCallum and Hocking 2005).
73 Resource-intensive strategies such as establishing captive breeding populations protected
74 from disease or translocating individuals to locations separated from infected populations
75 may also be justified (McCallum and Jones 2006). In contrast, if impacts are transitory, then a

76 preferred strategy may be to avoid interference to allow a new long-term endemic disease
77 state or pathogen extinction to be reached as quickly as possible (Gandon et al. 2013).
78 Longer-term evolutionary processes can operate to ultimately reduce the impact of the
79 disease on the host population (Fenner 1983, Kerr 2012), and inappropriate disease
80 management strategies may slow down evolution of both host and pathogen.

81 Models of infectious diseases in the early stages of emergence typically focus on
82 estimating R_0 , the number of secondarily infected individuals when one infected individual is
83 introduced into a wholly susceptible population (Lloyd-Smith et al. 2005). This is a key
84 parameter for devising strategies to limit invasion or control an outbreak because it allows the
85 estimation of vaccination or removal rates necessary to eradicate disease. However, by
86 definition, it does not include density dependent factors and is therefore sometimes
87 insufficient to predict the long-term consequences of disease introduction into a new
88 population (Heesterbeek 2002).

89 Most existing models for infectious disease are based around compartmental
90 Susceptible – Exposed – Infected – Recovered epidemiological models (S-E-I-R), which rely
91 on a strict assumption of homogeneity of individuals within compartments (Anderson and
92 May 1991). There is a parallel literature for macroparasitic infections, which assumes both a
93 stationary distribution of parasites amongst hosts and that parasite burden is determined by
94 the number of infective stages the host has encountered (Anderson and May 1978). For many
95 pathogens, pathogen load on (or inside) an individual typically changes following infection as
96 a result of within-host processes, causing temporal shifts in transmission and host mortality
97 rates. For example, the volume of transmissible tumours on Tasmanian devils (*Sarcophilus*
98 *harrisii*) increases through time, with measurable impacts on survival (Wells et al. 2017) and
99 likely temporal increases in transmission probability to uninfected devils that bite into the
100 growing tumour mass (Hamede et al. 2013). Similarly, increasing burden of the amphibian

101 chytrid fungus *Batrachochytrium dendrobatidis* on individual frogs after infection limits host
102 survival, with important consequences for disease spread and population dynamics (Briggs et
103 al. 2010, Wilber et al. 2016). Burdens of the causative agent of white nose syndrome,
104 *Pseudogymnoascus destructans*, which threatens numerous bat species in North America,
105 similarly increase on most individuals during the period of hibernation (Langwig et al. 2015).
106 The additional time dependence introduced by within-host pathogen growth can have a major
107 influence on the dynamics of host-pathogen interactions as uncovered by nested models that
108 link within- and between-host processes of disease dynamics (Gilchrist and Coombs 2006,
109 Mideo et al. 2008). Such dynamics are poorly captured by conventional compartmental and
110 macroparasite model structures. Thus, connecting across the scales of within- and between-
111 host dynamics remains a key challenge in understanding infectious disease epidemiology
112 (Gog et al. 2015).

113 Here we develop an individual-based model to explore the long-term impact of devil
114 facial tumour disease (DFTD), a transmissible cancer, on Tasmanian devil populations.
115 DFTD is a recently emerged infectious disease, first detected in 1996 in north-eastern
116 Tasmania (Hawkins et al. 2006). It is caused by a clonal cancerous cell line, which is
117 transmitted by direct transfer of live tumour cells when devils bite each other (Pearse and
118 Swift 2006, Jones et al. 2008, Hamede et al. 2013). DFTD is nearly always fatal and largely
119 affects individuals that are otherwise the fittest in the population (Wells et al. 2017).
120 Population declines to very low numbers concomitant with the frequency-dependent
121 transmission of DFTD led to predictions of devil extinctions, based on compartmental
122 epidemiological models (McCallum et al. 2009, Hamede et al. 2012).

123 Fortunately, the local devil extinctions predicted from these early models have not
124 occurred (McCallum et al. 2009). There is increasing evidence that rapid evolutionary
125 changes have taken place in infected devil populations, particularly in loci associated with

126 disease resistance and immune response (Epstein et al. 2016, Pye et al. 2016, Wright et al.
127 2017). Moreover, we recently reported that the force of infection (the rate at which
128 susceptible individuals become infected) increases over a time period of as long as six years
129 (~3 generations) after initial local disease emergence and that the time until death after initial
130 infection may be as long as two years (Wells et al. 2017). Therefore, despite high lethality,
131 the rate of epidemic increase appears to be relatively slow, prompting predictive modelling of
132 population level impacts over time spans well beyond those covered by field observations.

133 In general, there are three potential long-term outcomes of host-pathogen interactions:
134 host extinction, pathogen extirpation, and host-pathogen coexistence. To determine the
135 likelihood of each of these outcomes in a local population of Tasmanian devils, we used
136 individual-based simulation modelling (Fig. 1) and pattern matching, based on ten years of
137 existing field data, to project population trajectories for Tasmanian devil populations over
138 100 years following DFTD introduction.

139

140 MATERIALS AND METHODS

141 *Model framework*

142 We implemented a stochastic individual-based simulation model of coupled Tasmanian devil
143 (*Sarcophilus harrisi*) demography and devil facial tumour disease (DFDT) epidemiology. A
144 full model description with overview of design, concept, and details (Grimm et al. 2006) can
145 be found in Appendix S1. In brief, we aimed to simulate the impact of DFTD on Tasmanian
146 devil populations and validate 10^6 model scenarios of different random input parameters (26
147 model parameters assumed to be unknown and difficult or impossible to estimate from
148 empirical studies, see Appendix S1: Table S1) by matching known system level properties
149 (disease prevalence and population structure, see Appendix S1: Fig. S2) derived from a wild
150 population studied over ten years after the emergence of DFTD (Hamede et al. 2015). In

151 particular, running model scenarios for 100 years prior to, and after the introduction of
 152 DFTD, we explored the extent to which DFTD causes devil populations to decline or become
 153 extinct. Moreover, we aimed to explore whether input parameters such as the latency period
 154 of DFTD or the frequencies of disease transmission between individuals of different ages can
 155 be identified by matching simulation scenarios to field patterns of devil demography and
 156 disease prevalence.

157 Entities in the model are individuals that move in weekly time steps (movement
 158 distance θ) within their home ranges and may potentially engage in disease-transmitting
 159 biting behaviour with other individuals (Fig 1). Birth-death processes and DFTD
 160 epidemiology are modelled as probabilities according to specified input parameter values for
 161 each scenario. In each time step, processes are scheduled in the following order: 1)
 162 reproduction of mature individuals (if the week matches the reproductive season), 2)
 163 recruitment of juveniles into the population, 3) natural death (independent of DFTD), 4)
 164 physical interaction and potential disease transmission, 5) growth of tumours, 6) DFTD-
 165 induced death, 7) movement of individuals, 8) aging of individuals.

166 The force of infection $\lambda_{i,t}$, i.e. the probability that a susceptible individual i acquires
 167 DFTD at time t is given as the sum of the probabilities of DFTD being transmitted from any
 168 interacting infected individual k (with $k \in 1 \dots K$, with K being the number of all individuals in
 169 the population excluding i):

$$170 \quad \lambda_{i,t} = \left[\sum_{k \in K} \beta_{A(i)} \beta_{A(k)} \left(\frac{N_t}{C} \right)^\delta \left(\frac{1}{1+(1-r_{i,t})\omega} \right) \left(\frac{1}{1+(1-r_{k,t})\omega} \right) \left(\frac{V_{k,t}}{V_{max}} \right)^\gamma \right] I_\eta$$

171 Here, the disease transmission coefficient is composed of the two factors $\beta_{A(i)}$ and $\beta_{A(k)}$, each
 172 of which accounts for the age-specific interaction and disease transmission rate for
 173 individuals i and k according to their age classes A . N_t is the population size at time t and C is
 174 the carrying capacity of the study region; the scaling factor δ accounts for possible increase in

175 interactions frequency with increasing population size if $\delta > 0$. The parameter $r_{i,t}$ is a Boolean
 176 indicator of whether an individual recently reproduced and ω is a scaling factor that
 177 determines the difference in $\lambda_{i,t}$ resulting from interactions of reproductively active and non-
 178 reproducing individuals. $V_{k,t}$ is the tumour load of individual k , V_{max} is the maximum tumour
 179 load, and γ is a scaling factor of how $\lambda_{i,t}$ changes with tumour load of infected individuals.
 180 The parameter I_η is a Boolean indicator of whether two individuals are located in a spatial
 181 distance $< \eta$ that allows interaction and disease transmission (i.e. only individuals in
 182 distances $< \eta$ can infect each other). We considered individuals as ‘reproductively active’
 183 ($r_{i,t}=1$) for eight weeks after a reproduction event.

184 DFTD-induced mortality Ω_{size} (modelled as odds ratios in relation to demographic
 185 mortality rates with values between 0 and 1) accounts for tumour size, while tumour growth
 186 was modelled as a logistic function with the growth parameter α sampled as an input
 187 parameter. We allowed for latency periods τ between infection and the onset of tumour
 188 growth, which was also sampled as an input parameter. We assumed no recovery from
 189 DFTD, which appears to be very rare in the field (Pye et al. 2016).

190 Notably, sampled scaling factor values of zero for δ , ω , and γ correspond to model
 191 scenarios with homogeneous interaction frequencies and disease transmission rates
 192 independent of population size, reproductive status and tumour load, respectively, while
 193 values of $\eta = 21$ km assume that individuals can infect each other independent of spatial
 194 proximity (i.e. individuals across the entire study area can infect each other). The sampled
 195 parameter space included scenarios that omitted *i*) effects of tumour load on infection and
 196 survival propensity, *ii*) effect of spatial proximity on the force of infection between pairs of
 197 individuals and *iii*) both effects of tumour load and spatial proximity, in each of 1,000
 198 scenarios. This sampling design was used to explicitly assess the importance of modelling
 199 individual tumour load and space use for accurately representing the system dynamics.

200

201 *Model validation and summary*

202 To resolve the most realistic model structures and assumptions from a wide range of
203 possibilities and to compare simulation output with summary statistics from our case study (a
204 devil population at West Pencil Pine in western Tasmania) (Wells et al. 2017), we used
205 likelihood-free Approximate Bayesian Computation (ABC) for approximating the most likely
206 input parameter values, based on the distances between observed and simulated summary
207 statistics (Toni et al. 2009). We used the ‘*neuralnet*’ regression method in the R package *abc*
208 (Csillery et al. 2012). Prediction error was minimized by determining the most accurate
209 tolerance rate and corresponding number of scenarios considered as posterior (distribution of
210 parameter values from scenarios selected to best match empirical evidence according to
211 ABC) through a subsampling cross validation procedure as implemented in the *abc* package.
212 For this, leave-one-out cross validation was used to evaluate the out-of-sample accuracy of
213 parameter estimates (using a subset of 100 randomly selected simulated scenarios), with a
214 prediction error estimated for each input parameter (Csillery et al. 2012); this step facilitates
215 selecting the most accurate number of scenarios as a posterior sample. However, we are
216 aware that none of the scenarios selected as posterior samples entirely represents the true
217 system dynamics. We identified $n = 122$ scenarios (tolerance rate of 0.009, Appendix S1: Fig.
218 S2) as a reasonable posterior selection with minimized prediction error but sufficiently large
219 sample size to express uncertainty in estimates. The distribution of summary statistics was
220 tested against the summary statistics from our case study as a goodness of fit test, using the
221 ‘*gfit*’ function in the *abc* package (with a p-value of 0.37 indicating reasonable fit, Appendix
222 S1: Fig. S3, S4).

223 We generated key summary statistics from the case study, in which DFTD was
224 expected to have been introduced shortly before the onset of the study (Hamede et al. 2015),

225 and a pre-selection of simulation scenarios, in which juveniles never comprised > 50% of the
226 population, DFTD prevalence at end of 10-year-period was between 10 and 70%, and the age
227 of individuals with growing tumours was ≥ 52 weeks. Hereafter, we refer to ‘prevalence’ as
228 the proportion of free-ranging devils (individuals ≥ 35 weeks old) with tumours of sizes ≥ 0.1
229 cm^3 ; we do so to derive a measure of prevalence from simulations that is comparable to those
230 inferred from the 10 years of field data. Summary statistics were: 1) mean DFTD prevalence
231 over the course of 10 years, 2) mean DFTD prevalence in the 10th year only, 3)
232 autocorrelation value for prevalence values lagged over one time step (capturing short-term
233 changes in DFTD prevalence), 4) three coefficient estimates of a cubic regression model of
234 the smoothed ordered difference in DFTD prevalence (fitting 3rd order orthogonal
235 polynomials of time for smoothed prevalence values using the loess function in R with degree
236 of smoothing set to $\alpha = 0.75$ in order to capture the overall temporal changes in DFTD
237 prevalence), 5) phase in seasonal population fluctuations, calculated from sinusoidal model
238 fitted to the number of trappable individuals in different time steps (capturing population
239 fluctuations due to seasonal birth pulses), 6) regression coefficient of a linear model of the
240 changing proportions of individuals ≥ 3 years old in the trappable population over the course
241 of 10 years (accounting for the known shift in demographic structure; DFTD dispatches
242 mostly mature and reproductively active devils). Summary statistics for the simulations were
243 based on the 37 selected weekly time steps after the introduction of DFTD that matched the
244 time sequences of capture sessions in the case study, which included records in ca. three
245 months intervals (using the first 30 time steps only for population sizes, as the empirical
246 estimates from the last year of field data may be subject to data censoring bias). Overall,
247 these summary statistics aimed to describe general patterns rather than reproducing the exact
248 course of population and disease prevalence changes over time, given that real systems would
249 not repeat themselves for any given dynamics (Wood 2010). Additionally, unknown factors

250 not considered in the model may contribute to the observed temporal changes in devil
251 abundance and disease prevalence.

252 As results from our simulations, we considered the posterior distributions of the
253 selected input parameters (as adjusted parameter values according to the ABC approach
254 utilised) and calculated the frequency and timing of population or disease extirpation from
255 the 100 years of simulation after DFTD introduction of the selected scenarios. All simulations
256 and statistics were performed in R version 3.4.3 (R Development Core Team 2017). We used
257 wavelet analysis based on Morlet power spectra as implemented in the R package
258 *WaveletComp* (Roesch and Schmidbauer 2014) to identify possible periodicity at different
259 frequencies in the time series of population sizes (based on all free-ranging individuals) for
260 scenarios in which DFTD persisted at least 100 years.

261 For estimating the sensitivity of the three possible long-term outcomes (devil extirpation,
262 DFTD extirpation, coexistence) to variation in the posterior estimates of key parameters (i.e.
263 the likely parameter values obtained through the ABC approach), we used boosted regression
264 trees using the '*gbm.step*' routine (binomial error structure, learning rate of 0.001, tree
265 complexity of 5, k-fold cross-validation procedure) in the R package *dismo* (Elith et al.
266 2008). Similar approaches to global sensitivity analysis were recently applied to eco-
267 epidemiological models (Wells et al. 2015, Drawert et al. 2017).

268

269 RESULTS

270 For scenarios that best matched empirical mark-recapture data, 21% of posterior scenarios
271 (26 out of 122) led to devil population extirpation in timespans of 13 – 42 years (mean = 21,
272 SD = 8; ~7-21 generations) after introduction of DFTD (Fig. 2). In contrast, the disease was
273 lost in 57% of these posterior scenarios (69 out of 122), with disease extirpation taking place
274 11 – 100 years (mean = 29, SD = 22) post-introduction (Fig. 2). Loss of DFTD from local

275 populations therefore appears to be much more likely than devil population extirpation, given
276 no other factor than DFTD reducing devil vital rates. Moreover, fluctuations in host and
277 pathogen after the introduction of DFTD exhibited long-period oscillations in most cases
278 (Fig. 3). In the 27 selected scenarios in which DFTD persisted in populations for 100 years
279 after disease introduction, population size 80-100 years after disease introduction was smaller
280 and more variable (mean = 137, SD = 36) than population sizes prior to the introduction of
281 DFTD (mean = 285, SD = 3; Fig. 4). The average DFTD prevalence 80-100 years after
282 disease introduction remained < 40% (mean = 14%, SD = 4%; Fig. 4). Most wavelet power
283 spectra of these scenarios showed long-period oscillations over time periods between 261 –
284 1040 weeks (corresponding to 5 – 20 years) (Appendix S1: Fig. S5).

285 Inference of input parameters was only possible for some parameters, whereas 95%
286 credible intervals for most of the posterior distributions were not distinguishable from the
287 (uniformly) sampled priors. Notably, the posterior mode for the latency period (τ) was
288 estimated as 50.5 weeks (95% credible interval 48.5 – 52.6 weeks, for unadjusted parameters
289 values the 95% was 22.9 – 94.3 weeks), providing a first estimate of this latent parameter
290 from field data (Appendix S1: Fig. S6, Table S2). The posterior of the DFTD-induced
291 mortality factor (odds relative to un-diseased devils) for tumours < 50 cm³ ($\Omega_{<50}$) was
292 constrained to relatively large values (Appendix S1: Fig. S6), supporting empirical estimates
293 that small tumours are unlikely to cause significant mortality of devils. Posterior distributions
294 of weekly movement distances (θ) and the spatial distance over which disease-transmitting
295 interactions took place (η), in turn, allowed no clear estimates of these parameters (Appendix
296 S1: Fig. S6). Notably, the 122 scenarios selected as posteriors all explicitly accounted for the
297 effect of tumour load on infection and survival, while 90% of selected scenarios included
298 spatial proximity of individuals as influencing disease transmission (i.e. selected scenarios
299 comprised 110 models that included both the effect of tumour load and spatial proximity,

300 while 12 models included tumour load but not spatial proximity). Sensitivity analysis
301 revealed that the long-term outcomes of extinctions (DFTD or devils) versus coexistence
302 were dependent on a suite of parameters related to spatial aspects of transmission, density
303 dependence on transmission and disease progression on individual devils (Appendix S1: Fig.
304 S7, Fig. S8).

305

306 DISCUSSION

307 Our results suggest that DFTD will not necessarily cause local Tasmanian devil extinction or
308 even long-term major declines, whereas the extirpation of DFTD or coexistence/endemicity is
309 much more likely. In cases where DFTD persists in local devil populations in the long-term,
310 oscillations with relatively long periods (5-20 years, corresponding to 2-10 generations)
311 appear likely. These predictions are starkly different from those derived from previous
312 compartmental models, which considered all devils with detectable tumours to be equally
313 infectious and assumed exponentially distributed time delays. These models predicted
314 extinction (McCallum et al. 2009), as did models with more realistic gamma distributed time
315 delays or with delay-differential equations that incorporated field-derived parameter
316 estimates of transmission and mortality rates (Beeton and McCallum 2011). These previous
317 models, however, differ also from our approach in that they ignore spatial structure and do
318 not account for the uncertainty in unknown parameters such as disease-induced mortality and
319 disease transmission rates.

320 The predictions from our individually-based model, derived from 10 years of
321 observational data at our case study site (West Pencil Pine), are consistent with observations
322 now emerging from long-term field studies of the dynamics of Tasmanian devils and DFTD
323 (Lazenby et al. 2018). No Tasmanian devil population has yet become extinct – and
324 populations persist, albeit in low numbers, where disease has been present the longest (e.g., at

325 wukalina/Mount William National Park and at Freycinet, where DFTD emerged,
326 respectively, at least 21 and 17 years ago) (Epstein et al. 2016). Also, a considerable decline
327 in DFTD prevalence has been observed in recent years at Freycinet (Sebastien Comte,
328 unpublished data). These study sites did not contribute to the fitting of our model and at least
329 to some extent constitute an independent validation and test of the model predictions. Our
330 modelling results suggest that observed population dynamics of devils and DFTD do not
331 require evolutionary changes, although there is evidence of rapid evolution in disease-
332 burdened devil populations (Epstein et al. 2016) similar to rapid evolution in other vertebrates
333 when subjected to intense selection pressure (Christie et al. 2016, Campbell-Staton et al.
334 2017).

335 One of the differences between earlier models and those we present here is the
336 inclusion of tumour growth, with mortality and transmission rates that depend on individual
337 disease burden. Inclusion of burden-dependent dynamics results in additional and
338 qualitatively different time delays than those incorporated in previous models. Tumours take
339 time to grow before they have a major impact on host survival and become highly infectious
340 (Hamede et al. 2017, Wells et al. 2017). This slows the spread of DFTD and its impact on
341 devil population fluctuations. It also means that parameters estimated from field data, without
342 taking tumour growth into account, may not adequately represent the system dynamics
343 (McCallum et al. 2009).

344 McCallum et al. (2009) and Beeton & McCallum (2011) used an informal rejection
345 method to conclude that the observed dynamics were inconsistent with density-dependent
346 transmission, because, in an SEI (susceptible-exposed-infected) model framework, the
347 observed high prevalence coupled with population decline could only be derived assuming
348 frequency-dependent transmission. This led to predictions of devil extinction. In contrast, our
349 model, which includes spatial aspects of the dynamics in addition to tumour growth, suggests

350 that there is some density-dependence in transmission, as the posterior distribution for the
351 parameter describing density dependence δ has a mode close to 1 (Appendix S1: Fig. S6).
352 This density dependence may be important in contributing to the increased likelihood of devil
353 population persistence predicted by our model.

354 Our models suggest that documented dramatic population declines during the first 10
355 years or so of the DFTD epizootic may represent just the first peak of a classical epidemic
356 (Bailey 1975). Long-term predictions from our models suggest, however, that DFTD is a
357 slow burning disease with population changes governed by long-term oscillations.

358 It is well known, both from simple Lotka-Volterra models and from a range of
359 empirical studies, that consumer–resource interactions have a propensity to cycle, driven by
360 the time delays inherent in these systems (Murdoch et al. 2003). Disease burden-dependent
361 demographic and epidemiological parameters, together with burden growth within the host,
362 add additional time delays, both lengthening any oscillations and increasing the likelihood
363 that they will be maintained in the longer term. Apparently, such time-delays increase the
364 probability of host-pathogen coexistence, similar to predator-prey dynamics, rather than host
365 or pathogen extirpation. Grounded in theory and a reasonable body of modelling studies of
366 other wildlife diseases, disease-induced population extinction appears to be more generally an
367 exception rather than the rule, unless host populations are very small, or unless there are
368 reservoir species that are tolerant of infection (de Castro and Bolker 2005). Although we
369 found DFTD extirpation 11-100 years after its emergence to be more likely than devil-DFTD
370 coexistence, we believe that recognising the slow burning spread of DFTD and possible long-
371 term oscillations is of practical importance. If both DFTD extirpation and coexistence need to
372 be considered on decadal time spans, immediate management actions after disease emergence
373 and initial population declines are not necessarily essential, if the goal is to maintain presence
374 of devils, even with lower population densities in the case of coexistence (Fig. 4).

375

376 The approach we apply here – coupling the flexibility of individual-based models to account
377 for heterogeneity in disease burden and space use with Approximate Bayesian Computation
378 to match model outcomes with available empirical evidence – offers considerable potential
379 for making predictions regarding the population dynamics for other emerging diseases,
380 including those with more rapid eco-epidemiological dynamics (Toni et al. 2009, Beaumont
381 2010, Johnson and Briggs 2011, Wells et al. 2015). A fundamental problem in applying
382 modelling approaches to forecast the outcome of emerging infectious disease epidemics is the
383 need to estimate parameter values based on empirical data derived from the relatively early
384 stages of an epizootic, in the absence of retrospective knowledge (Heesterbeek et al. 2015,
385 Ferguson et al. 2016). Examples include estimating R_0 for SARS (Lipsitch et al. 2003) and
386 for the 2014-2015 Ebola epidemic in West Africa (Whitty et al. 2014, WHO Ebola Response
387 Team 2014) among others (LaDeau et al. 2011). In most of these cases, the objective is to
388 estimate parameters associated with the growth phase of the epidemic to assess the
389 effectiveness of interventions such as vaccination. The task we have addressed in this paper is
390 even more challenging – seeking to predict the long-term endemic behaviour of a pathogen
391 that is currently still in the early stages of emergence. We suggest that management efforts to
392 maintain devil populations in the face of DFTD should be guided by our changing
393 understanding of the long-term dynamics of the DFTD epidemic. Management efforts in wild
394 populations that solely aim to combat the impact of DFTD can be counterproductive if they
395 disrupt long-term eco-evolutionary dynamics that may eventually lead to endemicity with
396 stable devil populations. Our ability to predict future outcomes in the absence of management
397 actions require some caution as we cannot fully exclude the possibility that DFTD can cause
398 local population extinctions once populations are small, warranting future research. While
399 our findings emphasize the importance of accounting for individual tumour load for accurate

400 prediction and epidemiological modelling of DFTD dynamics, our inability to uncover the
401 exact role of devil spatial proximity on disease transmission means that further research is
402 necessary to understand relevant factors in disease spread.

403

404 The key management implication of our model is that "heroic" management interventions are
405 unlikely to be necessary to ensure persistence of Tasmanian devil populations with regard to
406 DFTD control. Given more information on immune-related or genetic variation in resistance,
407 the model could be modified to assess the value of interventions such as vaccination or
408 reintroduction of captive reared animals. At the same time, we believe that any management
409 actions should be subject to rigorous quantitative analysis to explore possible long-term
410 impacts. In particular, allocating resources and scientific endeavours to the management of
411 wildlife diseases such as DFTD should not disguise the fact that sufficiently large and
412 undisturbed natural environments are a vital prerequisite for wildlife to persist and eventually
413 cope with perturbations such as infectious diseases without human intervention.

414

415

416 ACKNOWLEDGMENTS

417 The study was funded by NSF grant DEB 1316549 and NIH grant R01 GM126563-01 as part
418 of the joint NIH-NSF-USDA Ecology and Evolution of Infectious Diseases Program, NIH
419 grant P30GM103324, the Australian Research Council Discovery (DP110102656), Future
420 Fellowship (FT100100250), DECRA (DE17010116) and Linkage (LP0561120, LP0989613)
421 Schemes, the Fulbright Scholarship Scheme, the Ian Potter Foundation, the Australian
422 Academy of Science (Margaret Middleton Fund), two grants from the Estate of W.V. Scott,
423 the National Geographic Society, the Mohammed bin Zayed Conservation Fund, the
424 Holsworth Wildlife Trust and three Eric Guiler Tasmanian Devil Research Grants through the

425 Save the Tasmanian Devil Appeal of the University of Tasmania Foundation. We are grateful
426 for all support during field work underpinning this modelling study: M. and C. Walsh,
427 Discovery Holidays Parks-Cradle Mountain National Park, and Forico Pty Ltd provided
428 logistic support and many volunteers helped with data collection (published previously).
429 Comments from Samuel Alizon and anonymous reviewers improved previous drafts.
430 K.W. conceived the idea of this study, carried out the analysis and wrote the first draft. All
431 authors interpreted results and contributed to revisions. All authors gave final approval for
432 publication.

433

434 DATA ACCESSIBILITY

435 Data and R code supporting the results are available as supporting material Data S1 (table of
436 summary statistics derived from empirical field study) and Data S2 (R Code for running
437 simulation and analysing the simulation outcomes).

438

439

440

441

442

443

444

445

446

447

448 LITERATURE CITED

- 449 Anderson, R. M., and R. M. May. 1978. Regulation and stability of host-parasite population
450 interactions: 1. regulatory processes. *Journal of Animal Ecology* 47:219-247.
- 451 Anderson, R. M., and R. M. May. 1991. *Infectious diseases of humans: dynamics and*
452 *control*. Oxford University Press, Oxford.
- 453 Bailey, N. T. J. 1975. *The mathematical theory of infectious diseases and its applications*. 2nd
454 edition. Charles Griffin.
- 455 Beaumont, M. A. 2010. Approximate Bayesian Computation in evolution and ecology.
456 *Annual Review of Ecology, Evolution, and Systematics* 41:379-406.
- 457 Beeton, N., and H. McCallum. 2011. Models predict that culling is not a feasible strategy to
458 prevent extinction of Tasmanian devils from facial tumour disease. *Journal of Applied*
459 *Ecology* 48:1315-1323.
- 460 Benton, T. G., S. J. Plaistow, and T. N. Coulson. 2006. Complex population dynamics and
461 complex causation: devils, details and demography. *Proceedings of the Royal Society*
462 *Biological Sciences Series B*. 273:1173-1181.
- 463 Briggs, C. J., R. A. Knapp, and V. T. Vredenburg. 2010. Enzootic and epizootic dynamics of
464 the chytrid fungal pathogen of amphibians. *Proceedings of the National Academy of*
465 *Sciences* 107:9695-9700.
- 466 Campbell-Staton, S. C., Z. A. Cheviron, N. Rochette, J. Catchen, J. B. Losos, and S. V.
467 Edwards. 2017. Winter storms drive rapid phenotypic, regulatory, and genomic shifts
468 in the green anole lizard. *Science* 357:495-498.
- 469 Cazelles, B., and S. Hales. 2006. Infectious diseases, climate influences, and nonstationarity.
470 *Plos Medicine* 3:e328.
- 471 Christie, M. R., M. L. Marine, S. E. Fox, R. A. French, and M. S. Blouin. 2016. A single
472 generation of domestication heritably alters the expression of hundreds of genes.
473 *Nature Communications* 7:10676.

- 474 Csillery, K., O. Francois, and M. G. B. Blum. 2012. abc: an R package for approximate
475 Bayesian computation (ABC). *Methods in Ecology and Evolution* 3:475-479.
- 476 de Castro, F., and B. Bolker. 2005. Mechanisms of disease-induced extinction. *Ecology*
477 *Letters* 8:117-126.
- 478 Drawert, B., M. Griesemer, L. R. Petzold, and C. J. Briggs. 2017. Using stochastic
479 epidemiological models to evaluate conservation strategies for endangered
480 amphibians. *Journal of the Royal Society Interface* 14.
- 481 Elith, J., J. R. Leathwick, and T. Hastie. 2008. A working guide to boosted regression trees.
482 *Journal of Animal Ecology* 77:802-813.
- 483 Epstein, B., M. Jones, R. Hamede, S. Hendricks, H. McCallum, E. P. Murchison, B.
484 Schönfeld, C. Wiench, P. Hohenlohe, and A. Storfer. 2016. Rapid evolutionary
485 response to a transmissible cancer in Tasmanian devils. *Nature Communications*
486 7:12684.
- 487 Fenner, F. 1983. Biological control as exemplified by smallpox eradication and myxomatosis.
488 *Proceedings of the Royal Society B: Biological Sciences* 218:259-285.
- 489 Ferguson, N. M., Z. M. Cucunubá, I. Dorigatti, G. L. Nedjati-Gilani, C. A. Donnelly, M.-G.
490 Basáñez, P. Nouvellet, and J. Lessler. 2016. Countering the Zika epidemic in Latin
491 America. *Science* 353:353-354.
- 492 Gandon, S., M. E. Hochberg, R. D. Holt, and T. Day. 2013. What limits the evolutionary
493 emergence of pathogens? *Philosophical Transactions of the Royal Society B:*
494 *Biological Sciences* 368.
- 495 Gilchrist, M. A., and D. Coombs. 2006. Evolution of virulence: interdependence, constraints,
496 and selection using nested models. *Theoretical Population Biology* 69:145-153.

- 497 Gog, J. R., L. Pellis, J. L. N. Wood, A. R. McLean, N. Arinaminpathy, and J. O. Lloyd-
498 Smith. 2015. Seven challenges in modeling pathogen dynamics within-host and across
499 scales. *Epidemics* 10:45-48.
- 500 Grimm, V., U. Berger, F. Bastiansen, S. Eliassen, V. Ginot, J. Giske, J. Goss-Custard, T.
501 Grand, S. K. Heinz, G. Huse, A. Huth, J. U. Jepsen, C. Jorgensen, W. M. Mooij, B.
502 Mueller, G. Pe'er, C. Piou, S. F. Railsback, A. M. Robbins, M. M. Robbins, E.
503 Rossmanith, N. Rueger, E. Strand, S. Souissi, R. A. Stillman, R. Vabo, U. Visser, and
504 D. L. DeAngelis. 2006. A standard protocol for describing individual-based and
505 agent-based models. *Ecological Modelling* 198:115-126.
- 506 Hamede, R., J. Bashford, M. Jones, and H. McCallum. 2012. Simulating devil facial tumour
507 disease outbreaks across empirically derived contact networks. *Journal of Applied*
508 *Ecology* 49:447-456.
- 509 Hamede, R. K., N. J. Beeton, S. Carver, and M. E. Jones. 2017. Untangling the model
510 muddle: empirical tumour growth in Tasmanian devil facial tumour disease. *Scientific*
511 *Reports* 7:6217.
- 512 Hamede, R. K., H. McCallum, and M. Jones. 2013. Biting injuries and transmission of
513 Tasmanian devil facial tumour disease. *Journal of Animal Ecology* 82:182-190.
- 514 Hamede, R. K., A.-M. Pearse, K. Swift, L. A. Barmuta, E. P. Murchison, and M. E. Jones.
515 2015. Transmissible cancer in Tasmanian devils: localized lineage replacement and
516 host population response. *Proceedings of the Royal Society of London B: Biological*
517 *Sciences* 282:20151468.
- 518 Hastings, A. 2004. Transients: the key to long-term ecological understanding? *Trends in*
519 *Ecology & Evolution* 19:39-45.
- 520 Hawkins, C. E., C. Baars, H. Hesterman, G. J. Hocking, M. E. Jones, B. Lazenby, D. Mann,
521 N. Mooney, D. Pemberton, S. Pyecroft, M. Restani, and J. Wiersma. 2006. Emerging

- 522 disease and population decline of an island endemic, the Tasmanian devil *Sarcophilus*
523 *harrisii*. *Biological Conservation* 131:307-324.
- 524 Heesterbeek, H., R. M. Anderson, V. Andreasen, S. Bansal, D. De Angelis, C. Dye, K. T. D.
525 Eames, W. J. Edmunds, S. D. W. Frost, S. Funk, T. D. Hollingsworth, T. House, V.
526 Isham, P. Klepac, J. Lessler, J. O. Lloyd-Smith, C. J. E. Metcalf, D. Mollison, L.
527 Pellis, J. R. C. Pulliam, M. G. Roberts, C. Viboud, and I. N. I. I. Collaboration. 2015.
528 Modeling infectious disease dynamics in the complex landscape of global health.
529 *Science* 347.
- 530 Heesterbeek, J. A. P. 2002. A brief history of R_0 and a recipe for its calculation. *Acta*
531 *Biotheoretica* 50:189-204.
- 532 Johnson, L. R., and C. J. Briggs. 2011. Parameter inference for an individual based model of
533 chytridiomycosis in frogs. *Journal of Theoretical Biology* 277:90-98.
- 534 Jones, M. E., A. Cockburn, R. Hamede, C. Hawkins, H. Hesterman, S. Lachish, D. Mann, H.
535 McCallum, and D. Pemberton. 2008. Life-history change in disease-ravaged
536 Tasmanian devil populations. *Proceedings of the National Academy of Sciences of*
537 *the United States of America* 105:10023-10027.
- 538 Kerr, P. J. 2012. Myxomatosis in Australia and Europe: a model for emerging infectious
539 diseases. *Antiviral Research* 93:387-415.
- 540 LaDeau, S. L., G. E. Glass, N. T. Hobbs, A. Latimer, and R. S. Ostfeld. 2011. Data-model
541 fusion to better understand emerging pathogens and improve infectious disease
542 forecasting. *Ecological Applications* 21:1443-1460.
- 543 Langwig, K. E., W. F. Frick, R. Reynolds, K. L. Parise, K. P. Drees, J. R. Hoyt, T. L. Cheng,
544 T. H. Kunz, J. T. Foster, and A. M. Kilpatrick. 2015. Host and pathogen ecology drive
545 the seasonal dynamics of a fungal disease, white-nose syndrome. *Proceedings of the*
546 *Royal Society B-Biological Sciences* 282.

- 547 Lazenby, B. T., M. W. Tobler, W. E. Brown, C. E. Hawkins, G. J. Hocking, F. Hume, S.
548 Huxtable, P. Iles, M. E. Jones, C. Lawrence, S. Thalmann, P. Wise, H. Williams, S.
549 Fox, and D. Pemberton. 2018. Density trends and demographic signals uncover the
550 long-term impact of transmissible cancer in Tasmanian devils. *Journal of Applied*
551 *Ecology*:n/a-n/a.
- 552 Lipsitch, M., T. Cohen, B. Cooper, J. M. Robins, S. Ma, L. James, G. Gopalakrishna, S. K.
553 Chew, C. C. Tan, M. H. Samore, D. Fisman, and M. Murray. 2003. Transmission
554 dynamics and control of severe acute respiratory syndrome. *Science* 300:1966-1970.
- 555 Lloyd-Smith, J. O., P. C. Cross, C. J. Briggs, M. Daugherty, W. M. Getz, J. Latto, M. S.
556 Sanchez, A. B. Smith, and A. Swei. 2005. Should we expect population thresholds for
557 wildlife disease? *Trends in Ecology & Evolution* 20:511-519.
- 558 McCallum, H., and B. A. Hocking. 2005. Reflecting on ethical and legal issues in wildlife
559 disease. *Bioethics* 19:336-347.
- 560 McCallum, H., and M. Jones. 2006. To lose both would look like carelessness: Tasmanian
561 devil facial tumour disease. *Plos Biology* 4:1671-1674.
- 562 McCallum, H., M. Jones, C. Hawkins, R. Hamede, S. Lachish, D. L. Sinn, N. Beeton, and B.
563 Lazenby. 2009. Transmission dynamics of Tasmanian devil facial tumor disease may
564 lead to disease-induced extinction. *Ecology* 90:3379-3392.
- 565 Mideo, N., S. Alizon, and T. Day. 2008. Linking within- and between-host dynamics in the
566 evolutionary epidemiology of infectious diseases. *Trends in Ecology & Evolution*
567 23:511-517.
- 568 Murdoch, W. W., C. J. Briggs, and R. M. Nisbet. 2003. *Consumer-resource dynamics*.
569 Princeton University Press.
- 570 Pearse, A. M., and K. Swift. 2006. Allograft theory: transmission of devil facial-tumour
571 disease. *Nature* 439:549-549.

- 572 Pye, R., R. Hamede, H. V. Siddle, A. Caldwell, G. W. Knowles, K. Swift, A. Kreiss, M. E.
573 Jones, A. B. Lyons, and G. M. Woods. 2016. Demonstration of immune responses
574 against devil facial tumour disease in wild Tasmanian devils. *Biology letters* 12.
- 575 R Development Core Team. 2017. R: A language and environment for statistical computing.
576 R Foundation for Statistical Computing, Vienna, Austria.
- 577 Roesch, A., and H. Schmidbauer. 2014. WaveletComp: computational wavelet analysis. R
578 package version 1.0.
- 579 Smith, K. F., K. Acevedo-Whitehouse, and A. B. Pedersen. 2009. The role of infectious
580 diseases in biological conservation. *Animal Conservation* 12:1-12.
- 581 Toni, T., D. Welch, N. Strelkowa, A. Ipsen, and M. P. H. Stumpf. 2009. Approximate
582 Bayesian computation scheme for parameter inference and model selection in
583 dynamical systems. *Journal of the Royal Society Interface* 6:187-202.
- 584 Wells, K., B. W. Brook, R. C. Lacy, G. J. Mutze, D. E. Peacock, R. G. Sinclair, N.
585 Schwensow, P. Cassey, R. B. O'Hara, and D. A. Fordham. 2015. Timing and severity
586 of immunizing diseases in rabbits is controlled by seasonal matching of host and
587 pathogen dynamics. *Journal of the Royal Society Interface* 12:20141184.
- 588 Wells, K., R. Hamede, D. H. Kerlin, A. Storfer, P. A. Hohenlohe, M. E. Jones, and H. I.
589 McCallum. 2017. Infection of the fittest: devil facial tumour disease has greatest
590 effect on individuals with highest reproductive output. *Ecology Letters* 20:770-778.
- 591 Whitty, C. J. M., J. Farrar, N. Ferguson, W. J. Edmunds, P. Piot, M. Leach, and S. C. Davies.
592 2014. Tough choices to reduce Ebola transmission. *Nature* 515:192-194.
- 593 WHO Ebola Response Team. 2014. Ebola virus disease in West Africa - the first 9 months of
594 the epidemic and forward projections. *New England Journal of Medicine* 371:1481-
595 1495.

- 596 Wilber, M. Q., K. E. Langwig, A. M. Kilpatrick, H. I. McCallum, and C. J. Briggs. 2016.
597 Integral projection models for host-parasite systems with an application to amphibian
598 chytrid fungus. *Methods in Ecology and Evolution* 10:1182–1194
- 599 Wood, S. N. 2010. Statistical inference for noisy nonlinear ecological dynamic systems.
600 *Nature* 466:1102–1104.
- 601 Wright, B., C. E. Willet, R. Hamede, M. Jones, K. Belov, and C. M. Wade. 2017. Variants in
602 the host genome may inhibit tumour growth in devil facial tumours: evidence from
603 genome-wide association. *Scientific Reports* 7:423.

604

605

606

607

608

609

610

611

612

613

614

615

616

617

618

619

620

621 **FIGURE CAPTION**

622 **Figure 1.** Illustrative overview of the individual-based model to explore long-term population
623 changes of a Tasmanian devil population burdened with devil facial tumour disease (DFTD).
624 Individuals are distributed in a study area. For every weekly time step seven different
625 processes are modelled, namely 1) the possible recruitment of young from females
626 (conditional on young survival during previous weaning time), 2) possible death independent
627 of disease status, 3) movement of individuals away from their home range centre, 4)
628 behavioural interaction between nearby individuals that may result in the transmission of
629 DFTD, 5) growth of DFTD tumours, 6) death of individuals resulting from DFTD, 7) aging
630 of individuals.

631

632 **Figure 2.** Frequency distributions of timespans of devil extirpation (upper panel) and devil
633 facial tumour disease (DFTD) extirpation (lower panel) presented as years after the
634 introduction of the disease into populations. Number of plotted scenarios correspond to those
635 for which extirpation events were recorded (26 and 69 out of 122 posterior samples,
636 respectively).

637

638 **Figure 3.** Examples of long-term devil and tumour dynamics. Scenario 1 is an example of
639 DFTD extirpation, and Scenario 2 is an example of coexistence. The upper panels show the
640 summarized population sizes (free-ranging individuals ≥ 35 weeks old) over 100 years (5,200
641 weeks) of simulations after the introduction of DFTD in the population, middle panels show
642 the respective wavelet power spectra, based on Morlet wavelet analysis. Red spectral colours
643 in the power spectra indicate strong periodicity over weekly time spans depicted on the y-axis
644 and the corresponding time during the course of simulations indicated on the x-axis; blue
645 spectral colours indicate weak periodicity. Ridges (black lines) of strongest periodicity often

646 indicate long-term oscillations > 500 weeks. Lower panels show the prevalence of DFTD
647 (growing tumour $\geq 0.1 \text{ cm}^3$) in the respective population.

648

649 **Figure 4.** Frequency distributions (count) of mean devil populations sizes (x axis, upper
650 panel) and mean devil facial tumour disease (DFTD) prevalence (x axis, lower panel) 80-100
651 years after disease introduction for those scenarios ($n = 27$) in which DFDT persisted for at
652 least 100 years. The light-grey vertical line in the upper panel indicates the mean population
653 sizes of simulated populations over 100 years prior to disease introduction.

654

655

656

657

658

659

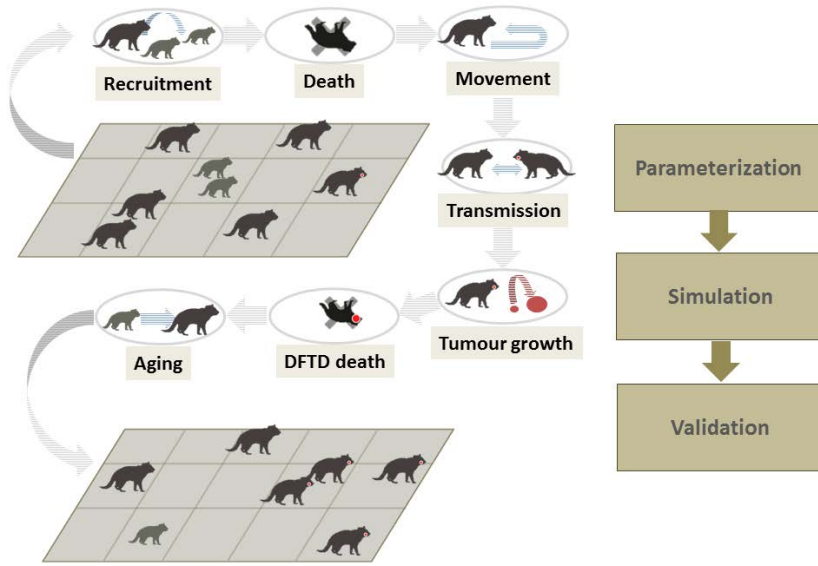
660

661

662

663

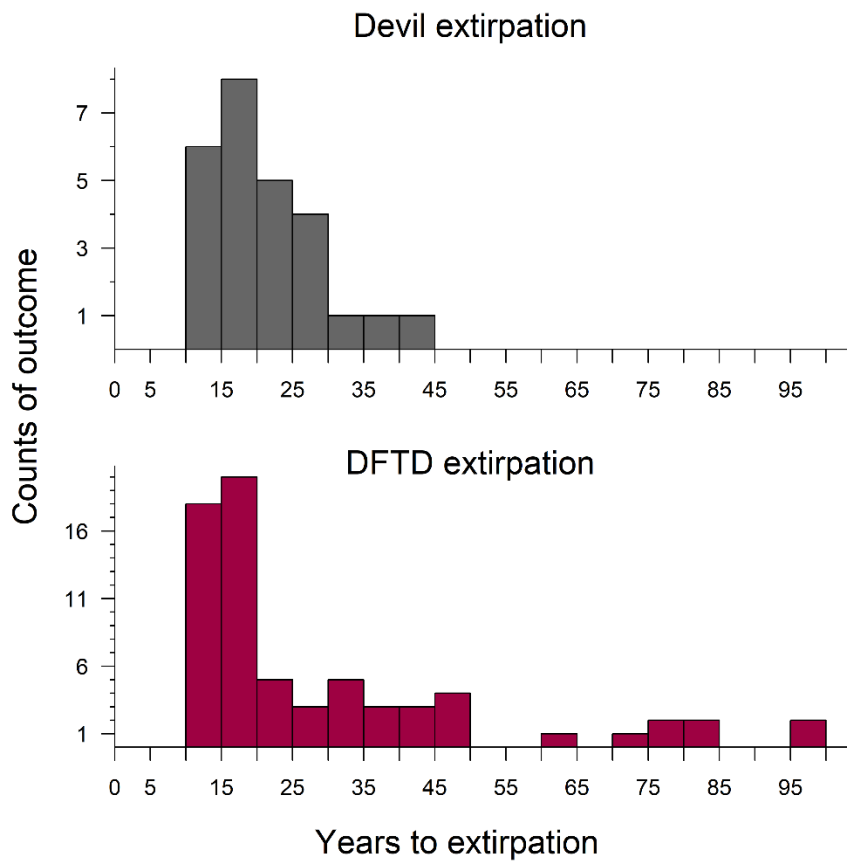
664



665

666 **Figure 1.**

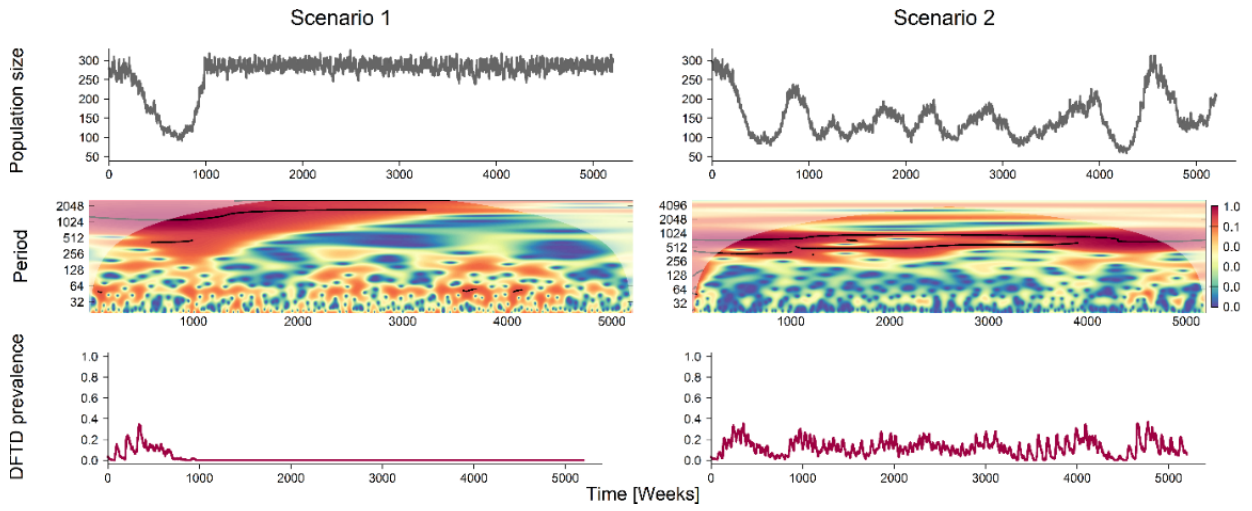
667



668

669 **Figure 2.**

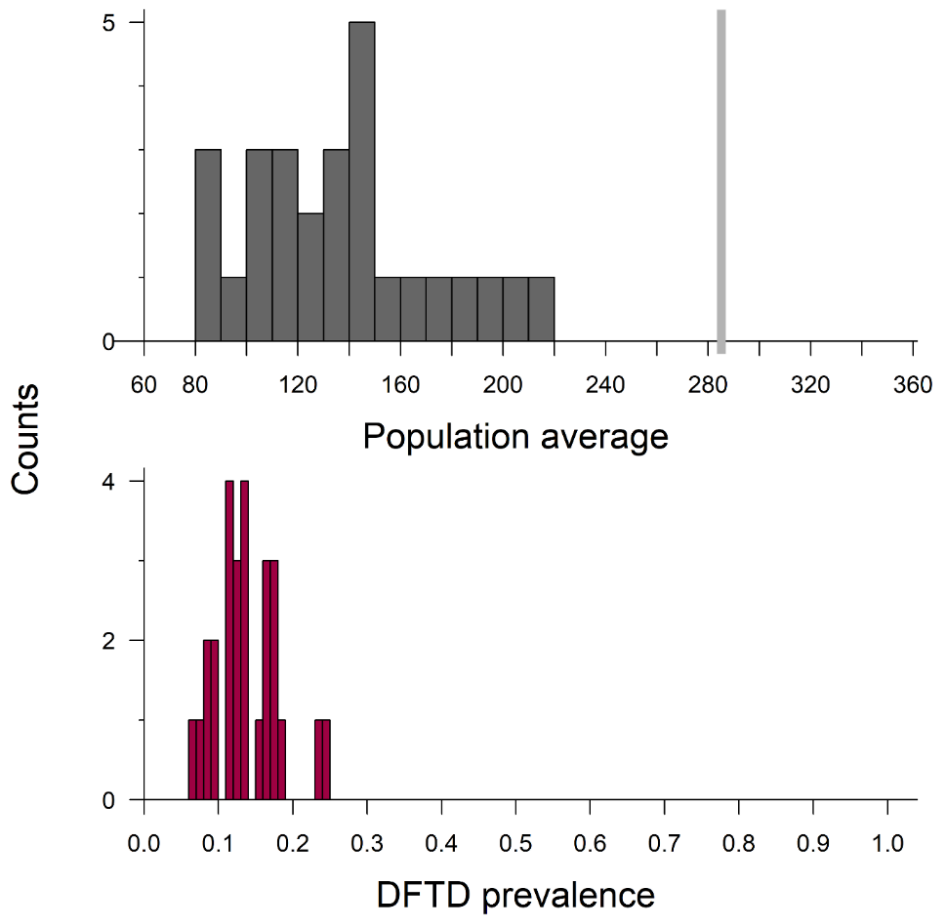
670



671

672 **Figure 3.**

673



674

675 **Figure 4.**